radicals, and nitric oxide, are a major contributor to oxidative stress. Cells protect against these effects of ROS with antioxidant enzymes. These results are consistent with those of previous studies reporting that RGC damage can be suppressed with antioxidant enzymes (Kong *et al.* 2007; Tanito *et al.* 2007; Munemasa *et al.* 2009; Koriyama *et al.* 2010). The present experimental model, NC, clearly induces oxidative stress, confirmed by the presence of oxidative stress markers such as 8-OHdG and 4HNE in the GCL. Keap1 was identified through a yeast two-hybrid screen. It suppresses Nrf2 activity by specifically binding to its evolutionarily conserved *N*-terminal Neh2 regulatory domain. When cysteine residues of Keap1 are modified by oxidative stress, the yeast two-hybrid screen changes. As a result, the suppression of Keap1 for Nrf2 is deactivated. Nrf2 subsequently translocates to the nucleus from the cytoplasm and activates the transcription of cytoprotective enzyme.

We found that RGCs in Nrf2 KO mice were more susceptible to NC-induced RGC death, and that the survival ratio of RGCs in the Nrf2 KO mice was lower than in WT mice both *in vivo* and *in vitro*. This is the first demonstration that Nrf2 plays a critical role in NC-induced RGC death. After NC, there is nuclear accumulation of Nrf2, and transcription of its downstream targets is activated, resulting in up-regulation of antioxidant and phase II detoxifying enzymes. After nuclear translocation of Nrf2, Tanito *et al.* observed significant up-regulation of antioxidant enzymes in a light exposure group (Tanito *et al.* 2007). He also reported that the up-regulation of antioxidants via the Keap1-Nrf2 pathway is very important in the mechanism of cytoprotection. Mitochondrial-derived death signaling has previously been reported to be an important pathway for RGC death induced by axonal damage (Chierzi *et al.* 1999; Qi *et al.* 2007). Mitochondria are also known to be abundant in the optic nerve (Barron *et al.* 2004). In this study, we detected ROS in the mitochondria of RGCs, suggesting that axonal damage affects mitochondrial function, triggering RGC death. Several studies of nerve-crushed RGCs have suggested that the caspase pathway in mitochondria plays a role in RGC death (Grosskreutz *et al.* 2005; Huang *et al.* 2005). Clinical studies of glaucoma have suggested that retinal microcirculation in the optic disc is disturbed in the early stages of the disease (Caprioli *et al.* 2010), and that as a result, axonal damage occurs in the lamina cribrosa. This axonal damage and mild chronic ischemia may induce ongoing oxidative stress in the axon and RGC body (Lieven *et al.* 2006). In this study, we have confirmed that oxidative stress is also involved in NC-induced RGC death. Oxidative stress induces ROS generation in mitochondria, causing the activation of Nrf2 (Calkins *et al.* 2005; Shih *et al.* 2005; Imhoff and Hansen 2009). Our results thus strongly suggest that the prevention of oxidative stress in mitochondria should be regarded as a candidate for the treatment of glaucoma.

In this study, we have also demonstrated that the activation of Nrf2 by CDDO-Im can protect against RGC death *in vivo*. To elucidate the effect of Nrf2 on RGC death after NC, we examined the expression of the Nrf2-responsive genes *Nqo1*, *Ho-1*, *Gclm*, *Gclc*, *Gsta4*, and *Txnrd*. We had assumed that the expression in the retina of *Nqo1*, one of the most important genes related to Nrf2 activation, would increase with time or the type of stimulation after injury. In addition, we have demonstrated that the expression of *Nqo1* and other antioxidant genes is up-regulated in WT mice treated with CDDO-Im, but not in Nrf2 KO mice. When Nrf2 was activated by CDDO-Im, a neuroprotective effect against NC-induced RGC death was also apparent *in vivo*. Antioxidant enzymes such as *Nqo1*, *Gclc*, and *Ho-1* protected the mitochondria from losing membrane potential and complex activity, and improved mitochondrial function (Feng *et al.* 2010). Our data thus suggest that Nrf2 plays a critical role in NC-induced RGC death. *Gclm* and *Gclc* did not change their expression after NC (as shown in Fig. 6), while CDDO-Im induced significant expression of *Gclm* and *Gclc* (as shown in Fig. 7). This CDDO-Im-induced expression did not occur in the Nrf2 KO mice. This would indicate that CDDO-Im has a stronger Nrf2-activating effect than NC, though further experiments are necessary to determine this.

Neuroprotective strategies have been proposed and are being investigated as new goals for glaucoma therapy. Effective neuroprotection, aimed at salvaging functional RGCs and their axons before they are irreversibly damaged, requires early intervention and the targeting of upstream events. Identification of the early clinical molecular events in RGC death would add to our understanding of the nature of glaucomatous injury and provide potential targets for neuroprotective strategies.

Acknowledgements

We thank Prof. Masao Ono (Department of Pathology, Tohoku University Graduate School of Medicine) and Dr. Takahiko Yamada (Yamada Takahiko Eye Clinic) for thoughtful comments, and Ms. Junko Sato and Ms. Natsumi Konno for technical assistance. We also thank Prof. Hideaki Hara and Dr. Masamitsu Shimazawa (Gifu Pharmaceutical University) for instruction on immunohistochemistry. This study was supported by Grants-in-Aid from the Ministry of Education, Science and Technology of Japan (23592613 for K.M). No other potential conflicts of interest relevant to this article were reported.

References

Aoki Y., Sato H., Nishimura N., Takahashi S., Itoh K. and Yamamoto M. (2001) Accelerated DNA adduct formation in the lung of the Nrf2 knockout mouse exposed to diesel exhaust. *Toxicol. Appl. Pharmacol.* **173**, 154–160.

Aoki Y., Hashimoto A. H., Amanuma K. *et al.* (2007) Enhanced spontaneous and benzo(a)pyrene-induced mutations in the lung of Nrf2-deficient gpt delta mice. *Cancer Res.* **67**, 5643–5648.

Bagnis A., Izzotti A. and Saccà S. C. (2012) Helicobacter pylori, oxidative stress and glaucoma. *Dig. Liver Dis.* **44**, 963–964.

Barron M. J., Griffiths P., Turnbull D. M., Bates D. and Nichols P. (2004) The distributions of mitochondria and sodium channels reflect the specific energy requirements and conduction properties of the human optic nerve head. *Br. J. Ophthalmol.* **88**, 286–290.

Calkins M. J., Jakel R. J., Johnson D. A., Chan K., Kan Y. W. and Johnson J. A. (2005) Protection from mitochondrial complex II inhibition in vitro and in vivo by Nrf2-mediated transcription. *Proc. Natl Acad. Sci. USA* **102**, 244–249.

Caprioli J., Coleman A. L., Discussion B. F. and i. G. (2010) Blood pressure, perfusion pressure, and glaucoma. *Am. J. Ophthalmol.* **149**, 704–712.

Chierzi S., Strettoi E., Cenni M. C. and Maffei L. (1999) Optic nerve crush: axonal responses in wild-type and bcl-2 transgenic mice. *J. Neurosci.* **19**, 8367–8376.

Choi D. H., Cristóvão A. C., Guhathakurta S., Lee J., Joh T. H., Beal M. F. and Kim Y. S. (2012) NADPH oxidase 1-mediated oxidative stress leads to dopamine neuron death in Parkinson's disease. *Antioxid. Redox Signal.* **16**, 1033–1045.

Clements C. M., McNally R. S., Conti B. J., Mak T. W. and Ting J. P. (2006) DJ-1, a cancer- and Parkinson's disease-associated protein, stabilizes the antioxidant transcriptional master regulator Nrf2. *Proc. Natl Acad. Sci. USA* **103**, 15091–15096.

Engin K. N., Yemişci B., Yiğit U., Ağaçhan A. and Coşkun C. (2010) Variability of serum oxidative stress biomarkers relative to biochemical data and clinical parameters of glaucoma patients. *Mol. Vis.* **16**, 1260–1271.

Enomoto A., Itoh K., Nagayoshi E., Haruta J., Kimura T., O'Connor T., Harada T. and Yamamoto M. (2001) High sensitivity of Nrf2 knockout mice to acetaminophen hepatotoxicity associated with decreased expression of ARE-regulated drug metabolizing enzymes and antioxidant genes. *Toxicol. Sci.* **59**, 169–177.

Feng Z., Liu Z., Li X., Jia H., Sun L., Tian C., Jia L. and Liu J. (2010) α-Tocopherol is an effective Phase II enzyme inducer: protective effects on acrolein-induced oxidative stress and mitochondrial dysfunction in human retinal pigment epithelial cells. *J. Nutr. Biochem.* **21**, 1222–1231.

Ferreira S. M., Lerner S. F., Brunzini R., Reides C. G., Evelson P. A. and Llesuy S. F. (2010) Time course changes of oxidative stress markers in a rat experimental glaucoma model. *Invest. Ophthalmol. Vis. Sci.* **51**, 4635–4640.

Fischer D., Petkova V., Thanos S. and Benowitz L. I. (2004) Switching mature retinal ganglion cells to a robust growth state in vivo: gene expression and synergy with RhoA inactivation. *J. Neurosci.* **24**, 8726–8740.

Grosskreutz C. L., Hänninen V. A., Pantcheva M. B., Huang W., Poulin N. R. and Dobberfuhl A. P. (2005) FK506 blocks activation of the intrinsic caspase cascade after optic nerve crush. *Exp. Eye Res.* **80**, 681–686.

Harada T., Harada C., Nakamura K. *et al.* (2007) The potential role of glutamate transporters in the pathogenesis of normal tension glaucoma. *J. Clin. Invest.* **117**, 1763–1770.

Hayreh S. S. (1997) Factors influencing blood flow in the optic nerve head. *J. Glaucoma* **6**, 412–425.

Huang W., Fileta J. B., Dobberfuhl A., Filippopolous T., Guo Y., Kwon G. and Grosskreutz C. L. (2005) Calcineurin cleavage is triggered by elevated intraocular pressure, and calcineurin inhibition blocks retinal ganglion cell death in experimental glaucoma. *Proc. Natl Acad. Sci. USA* **102**, 12242–12247.

Imhoff B. R. and Hansen J. M. (2009) Extracellular redox status regulates Nrf2 activation through mitochondrial reactive oxygen species. *Biochem. J.* **424**, 491–500.

Inokuchi Y., Imai S., Nakajima Y., Shimazawa M., Aihara M., Araie M. and Hara H. (2009) Edaravone, a free radical scavenger, protects against retinal damage in vitro and in vivo. *J. Pharmacol. Exp. Ther.* **329**, 687–698.

Inomata Y., Nakamura H., Tanito M., Teratani A., Kawaji T., Kondo N., Yodoi J. and Tanihara H. (2006) Thioredoxin inhibits NMDA-induced neurotoxicity in the rat retina. *J. Neurochem.* **98**, 372–385.

Itoh K., Chiba T., Takahashi S. *et al.* (1997) An Nrf2/small Maf heterodimer mediates the induction of phase II detoxifying enzyme genes through antioxidant response elements. *Biochem. Biophys. Res. Commun.* **236**, 313–322.

Iwase A., Suzuki Y., Araie M. *et al.* (2004) The prevalence of primary open-angle glaucoma in Japanese: the Tajimi Study. *Ophthalmology* **111**, 1641–1648.

Izzotti A., Bagnis A. and Saccà S. C. (2006) The role of oxidative stress in glaucoma. *Mutat. Res.* **612**, 105–114.

Kerr J., Nelson P. and O'Brien C. (1998) A comparison of ocular blood flow in untreated primary open-angle glaucoma and ocular hypertension. *Am. J. Ophthalmol.* **126**, 42–51.

Kong L., Tanito M., Huang Z., Li F., Zhou X., Zaharia A., Yodoi J., McGinnis J. F. and Cao W. (2007) Delay of photoreceptor degeneration in tubby mouse by sulforaphane. *J. Neurochem.* **101**, 1041–1052.

Koriyama Y., Chiba K., Yamazaki M., Suzuki H., Muramoto K. and Kato S. (2010) Long-acting genipin derivative protects retinal ganglion cells from oxidative stress models in vitro and in vivo through the Nrf2/antioxidant response element signaling pathway. *J. Neurochem.* **115**, 79–91.

Lee J., Kannagi M., Ferrante R. J., Kowall N. W. and Ryu H. (2009) Activation of Ets-2 by oxidative stress induces Bcl-xL expression and accounts for glial survival in amyotrophic lateral sclerosis. *FASEB J.* **23**, 1739–1749.

Liby K., Hock T., Yore M. M. *et al.* (2005) The synthetic triterpenoids, CDDO and CDDO-imidazolide, are potent inducers of heme oxygenase-1 and Nrf2/ARE signaling. *Cancer Res.* **65**, 4789–4798.

Lieven C. J., Hoegger M. J., Schlieve C. R. and Levin L. A. (2006) Retinal ganglion cell axotomy induces an increase in intracellular superoxide anion. *Invest. Ophthalmol. Vis. Sci.* **47**, 1477–1485.

Liu B. and Neufeld A. H. (2001) Nitric oxide synthase-2 in human optic nerve head astrocytes induced by elevated pressure in vitro. *Arch. Ophthalmol.* **119**, 240–245.

Maher P. and Hanneken A. (2005a) Flavonoids protect retinal ganglion cells from oxidative stress-induced death. *Invest. Ophthalmol. Vis. Sci.* **46**, 4796–4803.

Maher P. and Hanneken A. (2005b) The molecular basis of oxidative stress-induced cell death in an immortalized retinal ganglion cell line. *Invest. Ophthalmol. Vis. Sci.* **46**, 749–757.

Munemasa Y., Ahn J. H., Kwong J. M., Caprioli J. and Piri N. (2009) Redox proteins thioredoxin 1 and thioredoxin 2 support retinal ganglion cell survival in experimental glaucoma. *Gene Ther.* **16**, 17–25.

Nagai N., Thimmulappa R. K., Cano M. *et al.* (2009) Nrf2 is a critical modulator of the innate immune response in a model of uveitis. *Free Radic. Biol. Med.* **47**, 300–306.

Nakazawa T., Tamai M. and Mori N. (2002a) Brain-derived neurotrophic factor prevents axotomized retinal ganglion cell death through MAPK and PI3K signaling pathways. *Invest. Ophthalmol. Vis. Sci.* **43**, 3319–3326.

Nakazawa T., Tomita H., Yamaguchi K., Sato Y., Shimura M., Kuwahara S. and Tamai M. (2002b) Neuroprotective effect of nipradilol on axotomized rat retinal ganglion cells. *Curr. Eye Res.* **24**, 114–122.

Nakazawa T., Matsubara A., Noda K. *et al.* (2006a) Characterization of cytokine responses to retinal detachment in rats. *Mol. Vis.* **12**, 867–878.

Nakazawa T., Nakazawa C., Matsubara A. *et al.* (2006b) Tumor necrosis factor-alpha mediates oligodendrocyte death and delayed retinal ganglion cell loss in a mouse model of glaucoma. *J. Neurosci.* **26**, 12633–12641.

Nakazawa T., Hisatomi T., Nakazawa C. *et al.* (2007a) Monocyte chemoattractant protein 1 mediates retinal detachment-induced photoreceptor apoptosis. *Proc. Natl Acad. Sci. USA* **104**, 2425–2430.

Nakazawa T., Takahashi H., Nishijima K., Shimura M., Fuse N., Tamai M., Hafezi-Moghadam A. and Nishida K. (2007b) Pitavastatin prevents NMDA-induced retinal ganglion cell death by suppressing leukocyte recruitment. *J. Neurochem.* **100**, 1018–1031.

Neufeld A. H., Sawada A. and Becker B. (1999) Inhibition of nitric-oxide synthase 2 by aminoguanidine provides neuroprotection of retinal ganglion cells in a rat model of chronic glaucoma. *Proc. Natl Acad. Sci. USA* **96**, 9944–9948.

Osburn W. O. and Kensler T. W. (2008) Nrf2 signaling: an adaptive response pathway for protection against environmental toxic insults. *Mutat. Res.* **659**, 31–39.

Padmanabhan B., Tong K. I., Ohta T. *et al.* (2006) Structural basis for defects of Keap1 activity provoked by its point mutations in lung cancer. *Mol. Cell* **21**, 689–700.

Qi X., Lewin A. S., Sun L., Hauswirth W. W. and Guy J. (2007) Suppression of mitochondrial oxidative stress provides long-term neuroprotection in experimental optic neuritis. *Invest. Ophthalmol. Vis. Sci.* **48**, 681–691.

Quigley H. A. (1996) Number of people with glaucoma worldwide. *Br. J. Ophthalmol.* **80**, 389–393.

Ramamoorthy M., Sykora P., Scheibye-Knudsen M., Dunn C., Kasmer C., Zhang Y., Becker K. G., Croteau D. L. and Bohr V. A. (2012) Sporadic Alzheimer disease fibroblasts display an oxidative stress phenotype. *Free Radic. Biol. Med.* **53**, 1371–1380.

Ryu M., Yasuda M., Shi D. *et al.* (2012) Critical role of calpain in axonal damage-induced retinal ganglion cell death. *J. Neurosci. Res.* **90**, 802–815.

Salido E. M., de Zavalía N., Schreier L., De Laurentiis A., Rettori V., Chianelli M., Keller Sarmiento M. I., Arias P. and Rosenstein R. E. (2012) Retinal changes in an experimental model of early type 2 diabetes in rats characterized by non-fasting hyperglycemia. *Exp. Neurol.* **236**, 151–160.

Satoh T., Okamoto S. I., Cui J., Watanabe Y., Furuta K., Suzuki M., Tohyama K. and Lipton S. A. (2006) Activation of the Keap1/Nrf2 pathway for neuroprotection by electrophilic [correction of electrophillic] phase II inducers. *Proc. Natl Acad. Sci. USA* **103**, 768–773.

Seki M. and Lipton S. A. (2008) Targeting excitotoxic/free radical signaling pathways for therapeutic intervention in glaucoma. *Prog. Brain Res.* **173**, 495–510.

Shanab A. Y., Nakazawa T., Ryu M. *et al.* (2012) Metabolic stress response implicated in diabetic retinopathy: the role of calpain, and the therapeutic impact of calpain inhibitor. *Neurobiol. Dis.* **48**, 556–567.

Shareef S., Sawada A. and Neufeld A. H. (1999) Isoforms of nitric oxide synthase in the optic nerves of rat eyes with chronic moderately elevated intraocular pressure. *Invest. Ophthalmol. Vis. Sci.* **40**, 2884–2891.

Shih A. Y., Imbeault S., Barakauskas V., Erb H., Jiang L., Li P. and Murphy T. H. (2005) Induction of the Nrf2-driven antioxidant response confers neuroprotection during mitochondrial stress in vivo. *J. Biol. Chem.* **280**, 22925–22936.

Singh A., Misra V., Thimmulappa R. K. *et al.* (2006) Dysfunctional KEAP1-NRF2 interaction in non-small-cell lung cancer. *PLoS Med.* **3**, e420.

Sullivan R. K., Woldemussie E., Macnab L., Ruiz G. and Pow D. V. (2006) Evoked expression of the glutamate transporter GLT-1c in retinal ganglion cells in human glaucoma and in a rat model. *Invest. Ophthalmol. Vis. Sci.* **47**, 3853–3859.

Tanito M., Agbaga M. P. and Anderson R. E. (2007) Upregulation of thioredoxin system via Nrf2-antioxidant responsive element pathway in adaptive-retinal neuroprotection in vivo and in vitro. *Free Radic. Biol. Med.* **42**, 1838–1850.

Uno K., Prow T. W., Bhutto I. A., Yerrapureddy A., McLeod D. S., Yamamoto M., Reddy S. P. and Lutty G. A. (2010) Role of Nrf2 in retinal vascular development and the vaso-obliterative phase of oxygen-induced retinopathy. *Exp. Eye Res.* **90**, 493–500.

Vargas M. R., Johnson D. A., Sirkis D. W., Messing A. and Johnson J. A. (2008) Nrf2 activation in astrocytes protects against neurodegeneration in mouse models of familial amyotrophic lateral sclerosis. *J. Neurosci.* **28**, 13574–13581.

Vorwerk C. K., Gorla M. S. and Dreyer E. B. (1999) An experimental basis for implicating excitotoxicity in glaucomatous optic neuropathy. *Surv. Ophthalmol.* **43**(Suppl 1), S142–S150.

Yücel Y. H., Zhang Q., Weinreb R. N., Kaufman P. L. and Gupta N. (2003) Effects of retinal ganglion cell loss on magno-, parvo-, koniocellular pathways in the lateral geniculate nucleus and visual cortex in glaucoma. *Prog. Retin. Eye Res.* **22**, 465–481.

Zhao Z., Chen Y., Wang J., Sternberg P., Freeman M. L., Grossniklaus H. E. and Cai J. (2011) Age-related retinopathy in NRF2-deficient mice. *PLoS ONE* **6**, e19456.

Free Radical Biology and Medicine 61 (2013) 333–342

Contents lists available at SciVerse ScienceDirect

Free Radical Biology and Medicine

journal homepage: www.elsevier.com/locate/freeradbiomed

Original Contribution

The role of the Nrf2-mediated defense system in corneal epithelial wound healing

Ryuhei Hayashi [a,*,1], Noriko Himori [b,1], Keiko Taguchi [c], Yuki Ishikawa [a], Kohji Uesugi [a], Miyuki Ito [b], Thomas Duncan [a], Motokazu Tsujikawa [a], Toru Nakazawa [b], Masayuki Yamamoto [c], Kohji Nishida [a]

[a] Department of Ophthalmology, Osaka University School of Medicine, Suita, Osaka 565-0871, Japan
[b] Department of Ophthalmology and Tohoku University School of Medicine, Sendai, Japan
[c] Department of Medical Biochemistry, Tohoku University School of Medicine, Sendai, Japan

ARTICLE INFO

Article history:
Received 15 November 2012
Received in revised form
5 March 2013
Accepted 5 April 2013
Available online 12 April 2013

Keywords:
Nrf2
Keap1
Corneal epithelium
Wound healing
Cell migration
Cell proliferation
Free radicals

ABSTRACT

The corneal epithelium exists at the surface of cornea and is easily damaged by external stresses such as UV radiation or physical injury. The Nrf2-mediated defense system plays a central role in protecting cells by activating genes against these types of stress. In this study, we investigated the role of the Nrf2-mediated defense system in corneal epithelial wound healing by using Nrf2-knockout (KO) mice. Nrf2 was expressed in the corneal epithelium of wild-type (WT) mice, but not in KO mice. Observation of wounds after 24 h of healing revealed that healing of the corneal epithelium was significantly delayed in the Nrf2 KO mice, whereas Nrf2 was activated in the corneal epithelium of WT mice. Ki-67 staining revealed that the number of Ki-67-positive proliferating cells was significantly lower in the Nrf2 KO mice than in the WT mice at 24–36 h after injury; however, these numbers were approximately equivalent by 48 h. To clarify the role of Nrf2 during wound healing, we performed in vitro experiments with siRNA for Nrf2 and its suppressor Keap1. Nrf2 knockdown significantly delayed corneal epithelial cell migration, but did not affect cell proliferation. Conversely, Keap1 knockdown significantly accelerated cell migration. These results suggest that Nrf2 contributed to the corneal epithelial wound-healing process by accelerating cell migration, and Nrf2 would therefore be a good target for the treatment of corneal epithelial diseases such as dry eye or chronic corneal epithelial defect.

The cornea is a transparent tissue located in the anterior chamber of the eye. It consists of three layers—the epithelium, stroma, and endothelium. The corneal epithelium spans the entire surface of the cornea and plays a role in the defense of the ocular surface against external injury or infection. However, the corneal epithelium is easily damaged by external stresses such as UV radiation or physical injury. These external stresses have been known to involve oxidative stress [1–3], and the influence of oxidative stress on the corneal epithelium has been increasingly studied in recent years [4–7].

Additionally, whereas studies have discussed the effects of oxidative stress on corneal epithelium wound healing, they did not discuss the participation of the defense systems against oxidative stress. Thus, both the role and the mechanism of the defense system in corneal epithelial wound healing remain unclear.

The antioxidative stress factor Nrf2 is a transcriptional factor that systematically regulates the expression of various cytoprotective enzymes such as NAD(P)H dehydrogenase, quinone 1 (NQO1), heme oxygenase-1 (HO-1), and glutathione *S*-transferase [8–10]. Under normal conditions, Nrf2 is bound to Keap1 in the cytoplasm, and this complex is carried to proteasomes where it undergoes decomposition [11]. However, Nrf2 will dissociate from Keap1 when Keap1 is subjected to oxidative or electrophilic stress. After its translocation into nuclei, Nrf2 binds with the antioxidant response element and upregulates downstream genes [12,13]. Interestingly, recent studies have suggested that Nrf2 not only is involved in xenobiotic metabolism but also plays important roles in cancer generation and wound healing in some tissues [14–16]. However, neither the specific role nor the mechanism of action of the Nrf2-mediated defense system has been elucidated in wound-healing processes associated with the corneal epithelium or other tissues. Therefore, in this study, we attempted to clarify the role played by Nrf2 in corneal epithelial wound healing, migration, and proliferation by using Nrf2-knockout (KO) mice and Nrf2- or Keap1-specific small interfering RNA (siRNA).

Materials and methods

Animals

This study was performed in accordance with the ARVO *Statement for the Use of Animals in Ophthalmic and Vision Research* and was

* Corresponding author. Tel.: +81 6 6879 3453; fax: +81 6 6879 3458.
E-mail address: ryuhei.hayashi@ophthal.med.osaka-u.ac.jp (R. Hayashi).
[1] These authors contributed equally to this work.

0891-5849/$ - see front matter © 2013 Elsevier Inc. All rights reserved.
http://dx.doi.org/10.1016/j.freeradbiomed.2013.04.008

approved by the animal ethics and the recombinant DNA committees of Tohoku and Osaka University. Nrf2$^{-/-}$ mice were generated previously in our laboratory [12]. Wild-type (WT) ICR mice were purchased from Japan SLC (Shizuoka, Japan). Mice used in the wound-healing experiments were 7–14 weeks of age. All mice were genotyped for Nrf2 status by PCR amplification of genomic DNA extracted from tail tips. PCR amplification was performed using three different primers: 5′-TGGACGGGACTATTGAAGGCTG-3′ (sense for both genotypes), 5′-GCCGCCTTTTCAGTAGATGGAGG-3′ (antisense for WT), and 5′-GCGGATTGACCGTAATGGGATAGG-3′ (antisense for LacZ). All mice were allowed water and rodent chow ad libitum and subjected to an alternating 12-h (0800 to 2000 hours, 2000 to 0800 hours) light–dark cycle.

Table 1
Sequences of primers for RT-PCR.

Gene	Primer (5′ to 3′)
Nrf2	Forward: TGCCCCTCATCAGGCCCAGT
Nrf2	Reverse: GCTCGGCTGGGACTCGTGTT
Keap1	Forward: GGTGGCGCGCTGTGCTTAGT
Keap1	Reverse: TGCTGGCTCAGGCGAAGCTC
GAPDH	Forward: TCTGACGTGCCGCCTGGAGA
GAPDH	Reverse: GGGGTGGGTGGTCCAGGGTT

RT-PCR

Total RNA was obtained from corneal epithelium of WT and Nrf2 KO mice by using the RNeasy total RNA kit (Qiagen, Valencia, CA, USA). Reverse transcription was performed with the Super-Script First-Strand Synthesis System for RT-PCR (Invitrogen, Carlsbad, CA, USA), according to the manufacturer's suggested protocol, and cDNA was used as a template for PCR. The sequences of the primer pairs for Nrf2, Keap1, and GAPDH are presented in Table 1. The thermocycle program consisted of an initial cycle at 94 °C for 5 min and 28 cycles, for Nrf2 and GAPDH, and 32 cycles, for Keap1, at 94 °C for 30 s, 60 °C for 30 s, and 72 °C for 30 s (PCR thermal cycler MP; Takara Bio, Shiga, Japan).

Animal models for corneal epithelial wound healing

WT or Nrf2 KO mice were anesthetized by intramuscular injection of a mixture of ketamine (100 mg/kg) and xylazine (5 mg/kg). A circular piece of paper (2 mm in diameter) containing 0.2 μl *n*-heptanol was applied to the right eye of each of the Nrf2 KO ($n=12$) and WT mice ($n=10$) for 1 min [17]. The treated eyes were washed with 50 ml of saline, and Levofloxacin eye drops (Santen Pharmaceutical, Osaka, Japan) were administered to reduce the risk of bacterial contamination. The epithelial defect was stained with 1% fluorescein solution and photographed at 0, 6,

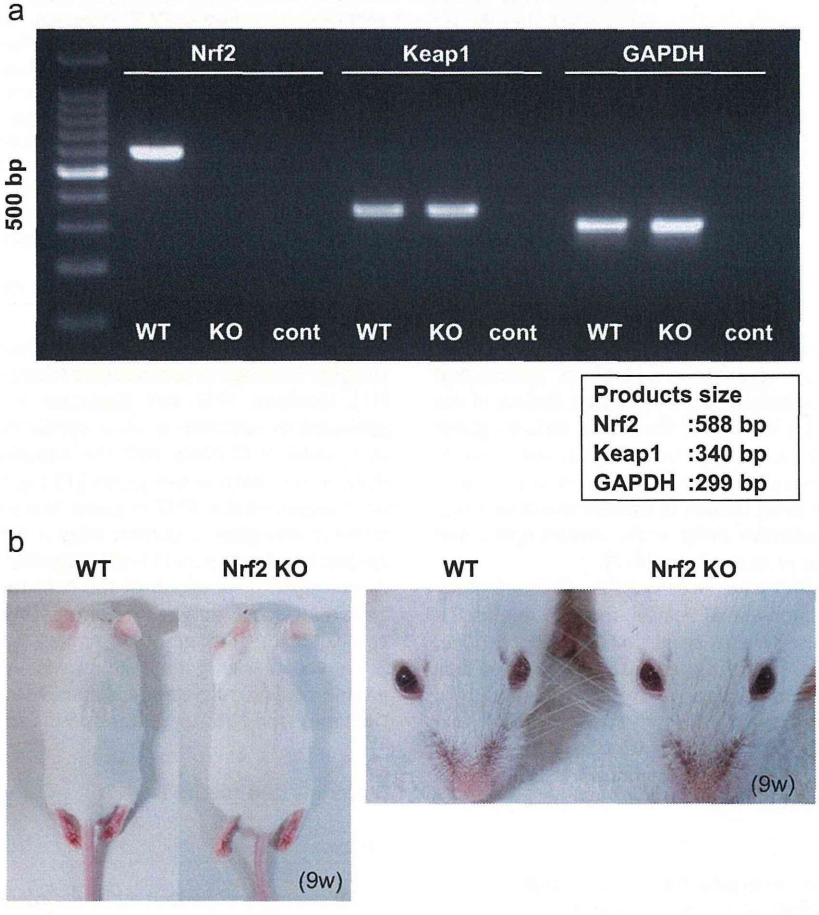

Fig. 1. Nrf2 and Keap1 mRNA expressions in corneal epithelium of WT and Nrf2 KO mice. (a) RT-PCR revealed that Nrf2 mRNA was expressed in the corneal epithelium of WT mice but not Nrf2 KO mice. Keap1, a binding partner of Nrf2, and GAPDH were expressed in the corneal epithelium of both WT and KO mice. The predicted product sizes for Nrf2, Keap1, and GAPDH were 588, 340, and 299 bp, respectively. (b) There was no apparent aberration in body size or cornea of Nrf2 KO mice compared to those of WT mice (9 weeks after birth).

12, 18, 24, 30, 36, 48, 60, and 72 h after epithelial debridement. The area of the epithelial defect was measured on photographs with a computer-assisted image analyzer (SL-7F; Topcon, Tokyo, Japan). Changes in the defect area were calculated (AxioVision; Carl Zeiss) and plotted on a graph. The experimental mice were euthanized by intraperitoneal injection of sodium pentobarbital solution, and then, the eyes were enucleated. Paraffin sections or frozen sections were processed for immunohistochemistry as described below.

Fluorescent immunostaining for Ki-67

Injured corneas healed at various time points were subjected to immunohistochemistry with Ki-67 antibody (ab15580; Abcam, Cambridge, MA, USA). The frozen corneoscleral tissue was cut into 10-μm-thick sections. After the sections were dried for 15 min at room temperature, they were fixed with cold methanol at −30 °C for 15 min and washed with Tris-buffered saline (TBS; Takara Bio) three times. For Ki-67 staining, slides were incubated with TBS containing 5% donkey serum and 0.3% Triton X for 1 h to block nonspecific reactions. The slides were incubated at 4 °C overnight with a 1:100 dilution of anti-Ki-67 antibody. The slides were again washed three times with TBS and incubated with a 1:200 dilution of Alexa Fluor 488-conjugated secondary antibody (Molecular Probes, Eugene, OR, USA). All tissue sections were counterstained with Hoechst 33342 and then examined under a microscope (Axiovert200M; Carl Zeiss). The total number of Ki-67-positive cells in each section was counted. The length of the basement membrane from limbus to limbus was measured for the cornea, and the number of Ki-67-positive cells per 100-μm basement membrane was calculated.

Hematoxylin and eosin staining and diaminobenzidine immunostaining for Nrf2

Each eye sample was fixed in formalin and embedded in paraffin. The slides were stained with hematoxylin and eosin (HE). For Nrf2 immunostaining, slides were treated with anti-Nrf2 antibody (produced in our laboratory), and positive reactivity was visualized through sequential incubation with biotinylated anti-rat IgG, streptavidin-conjugated horseradish peroxidase, and diaminobenzidine for staining. Hematoxylin was used for nuclear counterstaining.

siRNA-dependent specific knockdown of Nrf2 or Keap1 in TERT-immortalized human corneal epithelial cells (C/TERTs)

C/TERTs were obtained from the Harvard Skin Disease Research Center. C/TERTs were cultured in keratinocyte serum-free medium (KSFM) (Gibco Invitrogen). The siRNA (Nrf2, ID: s9491, and Keap, ID: s18981) and introducing reagent were purchased from Ambion (Austin, TX, USA) and Invitrogen, respectively. Nrf2- or Keap1-specific siRNA and control scramble siRNA (negative control) were introduced into C/TERTs with the introducing reagent for 18 h, after which the medium containing siRNA was removed and fresh medium was added. The total RNA of C/TERTs was collected each day to confirm Nrf2 or Keap1 knockdown by real-time PCR.

Cell migration assay

Migration assays were performed according to the manufacturer's protocol (Oris cell migration assay kit; Platypus Technologies, Madison, WI, USA) [18,19]. Briefly, each of the Nrf2-specific,

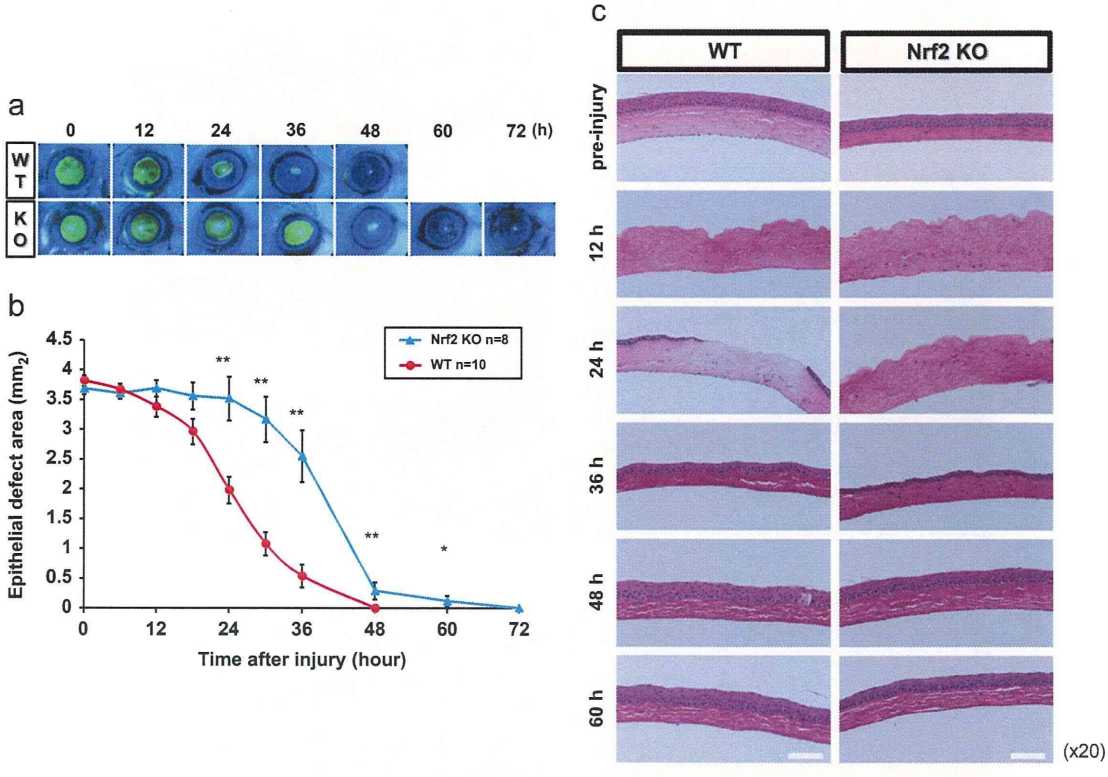

Fig. 2. Corneal epithelial wound healing in WT and Nrf2 KO mice. (a) The corneal epithelial layers of WT or Nrf2 KO mice were removed from the stroma by *n*-heptanol treatment. Epithelial defect regions were stained by fluorescein. The areas of the wounds were initially calculated and then (b) recalculated at various times after the injury. (c) HE staining was also performed at each time point. In WT mice, the closure of the corneal epithelial defect was completed within 48 h after the injury. Corneal epithelial wound healing was significantly delayed for 24 h or more in the Nrf2 KO mice compared with the WT mice. The graphs represent the means ± SE of 8–10 independent samples. $^{*}p < 0.05$, $^{**}p < 0.01$ (12, 24 h. *t* test; 35, 48, 60 h, Mann–Whitney *U*). Scale bars, 50 μm.

Keap1-specific, and control siRNA-introduced corneal epithelial cells was seeded outside of the partition in each well of a 96-well plate, and the partitions were subsequently removed. After 8 (Keap1 knockdown) or 24 h (Nrf2 knockdown), the migrated cells in the central parts of the wells were stained with calcein-AM; the fluorescence intensity was then measured by a fluorescence plate reader (ARVO MX; PerkinElmer, Norwalk, CT, USA). For the evaluation of the total cell number, all of the cells in the well were stained with Alamar blue (AbD Serotec, Oxford, UK) and the fluorescence signals were assessed by a fluorescence plate reader in each period.

Cell proliferation assay

Cell proliferation was evaluated by Alamar blue assay. The Nrf2-specific and Keap1-specific corneal epithelial cells as well as control corneal epithelial cells into which siRNA was introduced were seeded in each well of a 12-well plate and cultured in KSFM without growth factors. The Alamar blue assay was subsequently performed at 6, 24, 48, and 72 h.

Real-time RT-PCR

Total RNA was obtained from Nrf2-specific or control siRNA-introduced C/TERTs, and the cDNA was synthesized as a template for PCR. Quantitative real-time RT-PCR was performed using the ABI Prism 7500 fast sequence detection system (Applied Biosystems, Foster City, CA, USA), according to the manufacturer's suggested protocol. Primer pairs and TaqMan MGB probes labeled with 6-carboxyfluorescein at the 5′-end and nonfluorescent quencher at the 3′-end were designed using Assay-by-Design (Applied Biosystems; GAPDH, Hs99999905_m1; Nrf2, Hs00232352_m1; NQO1, Hs0016-8547_m1; HO-1, Hs01110250_m1; and Keap1, Hs00202227_m1). Thermocycling programs consisted of an initial cycle at 50 °C for 2 min and 95 °C for 10 min and 45 cycles at 95 °C for 15 s and 60 °C for 1 min. All assays were run in duplicate for four or more individual samples.

Statistical analysis

Data were expressed as means ± SE. Statistical analysis was performed with Student's t test or the Mann–Whitney rank sum test. Differences were considered significant at $p < 0.05$. All statistics were calculated using SigmaPlot 11.0 (Systat Software, San Jose, CA, USA).

Results

Nrf2 and Keap1 expression in WT and Nrf2 KO mice

To examine the expression of Nrf2 mRNA and its binding partner Keap1 mRNA in the corneal epithelium of Nrf2 KO and WT mice, we performed RT-PCR for the genes encoding Nrf2 and Keap1. The results indicate that Nrf2 mRNA was expressed in the corneal epithelium of WT mice but not Nrf2 KO mice. In contrast, Keap1 mRNA was expressed in both WT and Nrf2 KO mice (Fig. 1a).

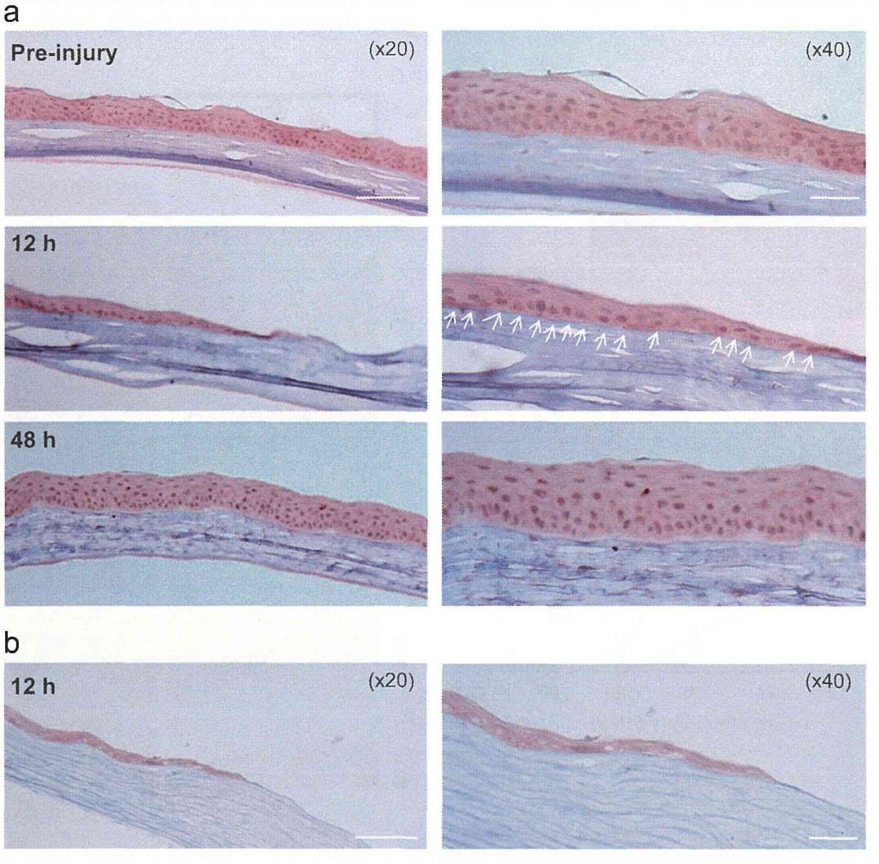

Fig. 3. Nrf2 activation in corneal epithelium during wound healing. Paraffin-embedded tissue sections were stained with anit-Nrf2 antibody to examine Nrf2 activation based on their translocation to the nuclei. (a) Nrf2 protein was expressed and located in the nuclei of preinjured corneal epithelia of WT mice (preinjury). During corneal epithelial wound healing, Nrf2 protein was also found in the corneal epithelium (12 and 48 h after injury, arrows indicate Nrf2-positive nuclei). (b) In Nrf2 KO mice, no signal for Nrf2 protein was detected in the corneal epithelium. Scale bars, 50 μm (20× original magnification) or 20 μm (40× original magnification).

There was no remarkable aberration in body size or eye of Nrf2 KO mice compared to those of WT mice (Fig. 1b).

Corneal epithelial wound healing in WT and Nrf2 KO mice

We compared the process of corneal epithelial wound healing in WT and Nrf2 KO mice to assess the involvement of Nrf2 in the wound-healing process. Immediately after corneal epithelial injury (0 h), no significant difference ($p=0.326$, t test) was observed in the area of the wound between the WT ($3.8 \pm 0.08\ mm^2$) and the Nrf2 KO ($3.7 \pm 0.10\ mm^2$) mice. In the WT mice, approximately 50% of the defect was resurfaced 24 h after injury, and no defect was observed 48 h after the injury (Figs. 2a and b). In contrast, the corneal epithelium of Nrf2 KO mice showed no sign of healing until 24 h after injury. The epithelial defect was gradually resurfaced between 24 and 48 h after injury in the Nrf2 KO mice, but the wound area was not completely healed until 48–60 h after the initial injury. The wound healing delay in the Nrf2 KO mice compared to the WT mice, after 24 h of wound healing, was statistically significant.

Histochemical analysis

HE staining showed that in the WT mice, corneal epithelial migration had already begun 24 h after injury in the central part of the cornea (Fig. 2c, WT). By 36 h, the corneal surface was covered by migrated corneal epithelial cells and epithelial stratification had commenced. By 48 h, four or five layers of corneal epithelium were fully reconstructed, in a state similar to the preinjured cornea. Conversely, in the Nrf2 KO mice, few corneal epithelial cells were observed in the central cornea even at 24 h after injury, suggesting a delay in cell migration in the Nrf2 KO mice (Fig. 2c, Nrf2 KO). At 36 h, the corneal surface was covered with one or two layers of migrated corneal epithelium (Fig. 3). By 48 h, the migrated corneal epithelium was stratified, and by 60–72 h, the corneal surface of Nrf2 KO mice appeared to be completely reconstructed, similar to the WT mice. These data demonstrate a delay in early cell migration 12–36 h after injury in the Nrf2 KO mice.

Activation of Nrf2 during corneal epithelial wound healing of WT mice

Nrf2 translocation to nuclei in the WT mice was evaluated by immunostaining to verify whether Nrf2 was activated during corneal epithelial wound healing. The results indicate that Nrf2 was present in the nuclei of preinjured corneal epithelial cells and also in the corneas of the WT mice at 12 and 48 h after injury (Fig. 3a), thus demonstrating that Nrf2 signaling was activated throughout the corneal epithelial wound-healing process.

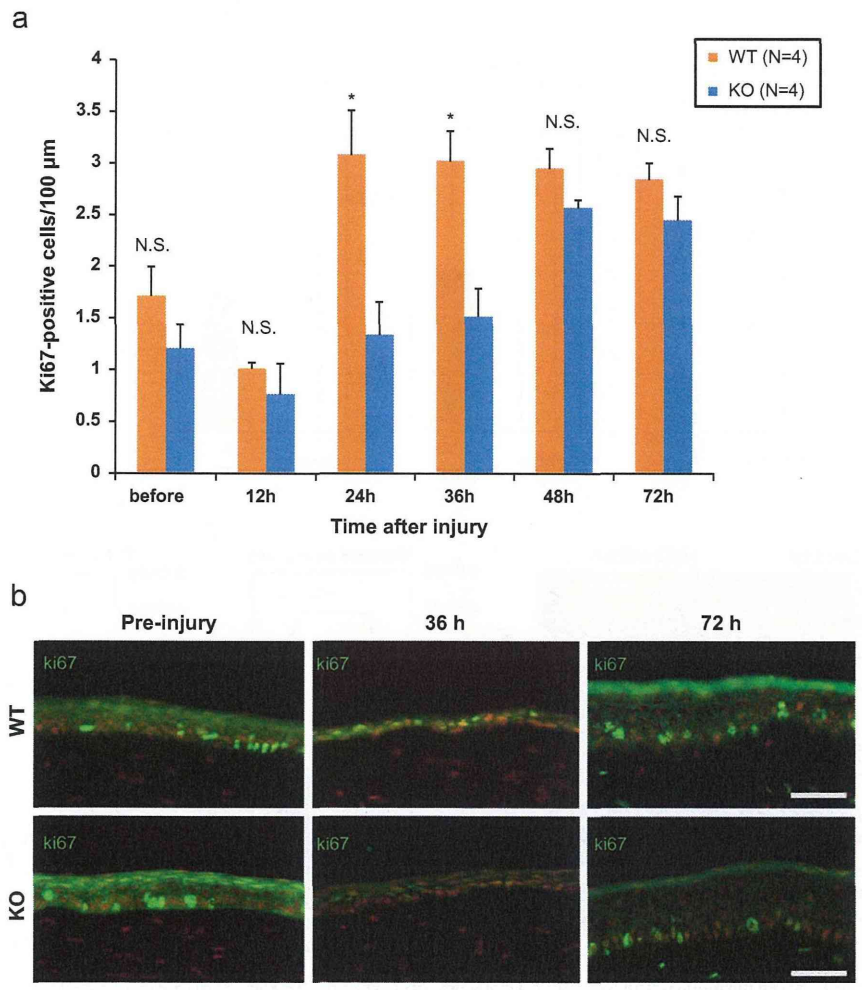

Fig. 4. Proliferative cells in WT and Nrf2 KO mice during corneal epithelial wound healing. (a and b) To assess cell proliferation in corneal epithelium in WT and Nrf2 KO mice, we performed Ki-67 staining at various times after the injury. Immunostaining revealed that at 24 and 36 h after injury, the number of Ki-67-positive cells in the Nrf2 KO mice was significantly reduced compared with that in the WT mice, whereas no significant difference was observed in the preinjured corneas and the injured corneas at 48–72 h after injury. The graphs represent the means ± SE of four independent samples. $^*p < 0.05$ (t test). Scale bars, 50 μm.

In contrast, no significant signal was observed in the nuclei of the corneal epithelium in Nrf2 KO mice (Fig. 3b).

Immunostaining for Ki-67 in corneal epithelium of WT and Nrf2 KO mice

To examine cell proliferation of the corneal epithelium during wound healing, we performed immunostaining for the proliferative marker Ki-67 in WT and Nrf2 KO mice. The results indicate that the numbers of Ki-67-positive proliferating cells in the Nrf2 KO mice transiently decreased at 24 and 36 h after injury. However, these values were nearly identical to those observed in the WT mice by 48 h after the injury (Figs. 4a and b), indicating that the proliferation was initiated later in the Nrf2 KO mice compared to the WT mice. Thus, Nrf2 probably affects the early migration process of corneal epithelial wound healing rather than cell proliferation.

The effects of Nrf2 knockdown on cell migration of corneal epithelial cells

To clarify the involvement of Nrf2 in cell migration in corneal epithelial wound healing, we performed Nrf2-specific knockdown by siRNA in a corneal epithelial cell line (C/TERT) in vitro. Over 70% of Nrf2 expression was suppressed by Nrf2-specific siRNA in C/TERT in vitro (76.6%, Fig. 5a). Furthermore, Nrf2-targeted siRNA significantly downregulated the Nfr2 downstream genes such as NQO1 (38.4%) and HO-1 (41.7%), indicating that Nrf2-mediated signal transduction was functionally suppressed by Nrf2 siRNA. The results of the migration assay revealed that Nrf2 suppression induced a significant reduction in the migration capability of C/TERTs (42.1%, Fig. 5b). Results of the Alamar blue assay indicated no significant difference in total cell number between the samples (Fig. 5c). These data indicate that Nrf2 knockdown in corneal epithelial cells affects cell migration capability.

The effects of Nrf2 activation throughout Keap1 knockdown on cell migration of corneal epithelial cells

To examine the effect of Nrf2 activation on cell migration, the Nrf2 suppressor Keap1 was knocked down by Keap1-targeted siRNA. The results of this experiment indicate that more than 70% of Keap1 expression was significantly suppressed by Keap1-specific siRNA in C/TERTs in vitro (Fig. 6a). In addition, Keap1-targeted siRNA significantly upregulated NQO1 (52.0%) and HO-1 (60.3%) but did not affect Nrf2 expression. This finding indicates that Nrf2 translocation to the nuclei was promoted and that Nrf2 was functionally activated by Keap1 siRNA. The results of the migration assay indicate that Keap1 suppression induces a significant increase in the migration capability of C/TERTs (214% increase, Fig. 6b). Similar to Nrf2 suppression, Keap1 suppression had no significant effect on the total number of C/TERT cells in this assay (Fig. 6c).

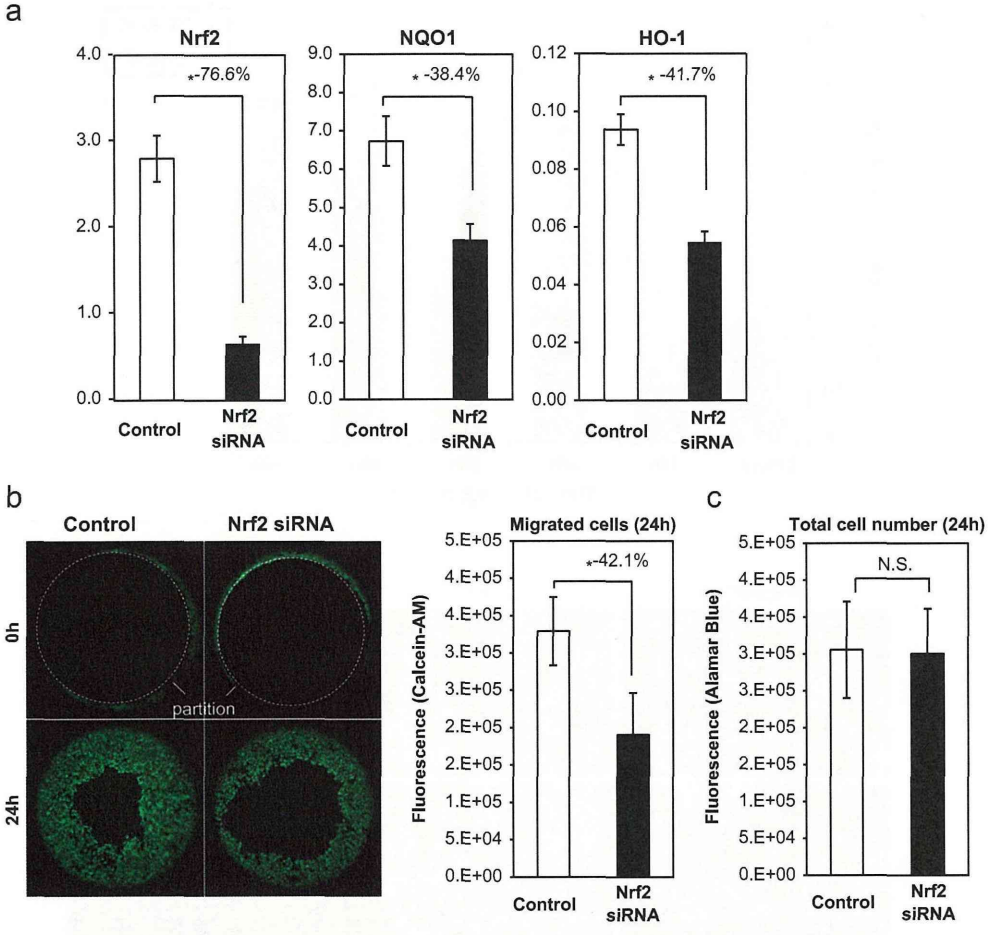

Fig. 5. The effect of Nrf2 knockdown on cell migration capability in corneal epithelial cells in vitro. (a) The effect of Nrf2-specific knockdown on the migration capability of C/TERT cells was examined; 76.6% of Nrf2 mRNA expression in C/TERT cells was suppressed by Nrf2-specific siRNA. Nrf2 knockdown also resulted in significant downregulation of its downstream genes, NQO1 and HO-1 (38.4 and 41.7%, respectively). (b) Nrf2- or control siRNA-introduced cells were allowed to migrate for 24 h and then stained with calcein-AM. The migration assay indicated that cell migration capability was significantly reduced by Nrf2 knockdown. (c) The Alamar Blue assay revealed no significant difference in the total cell number between the samples. The graphs represent the means ± SE of five independent samples. $^*p < 0.05$ (t test).

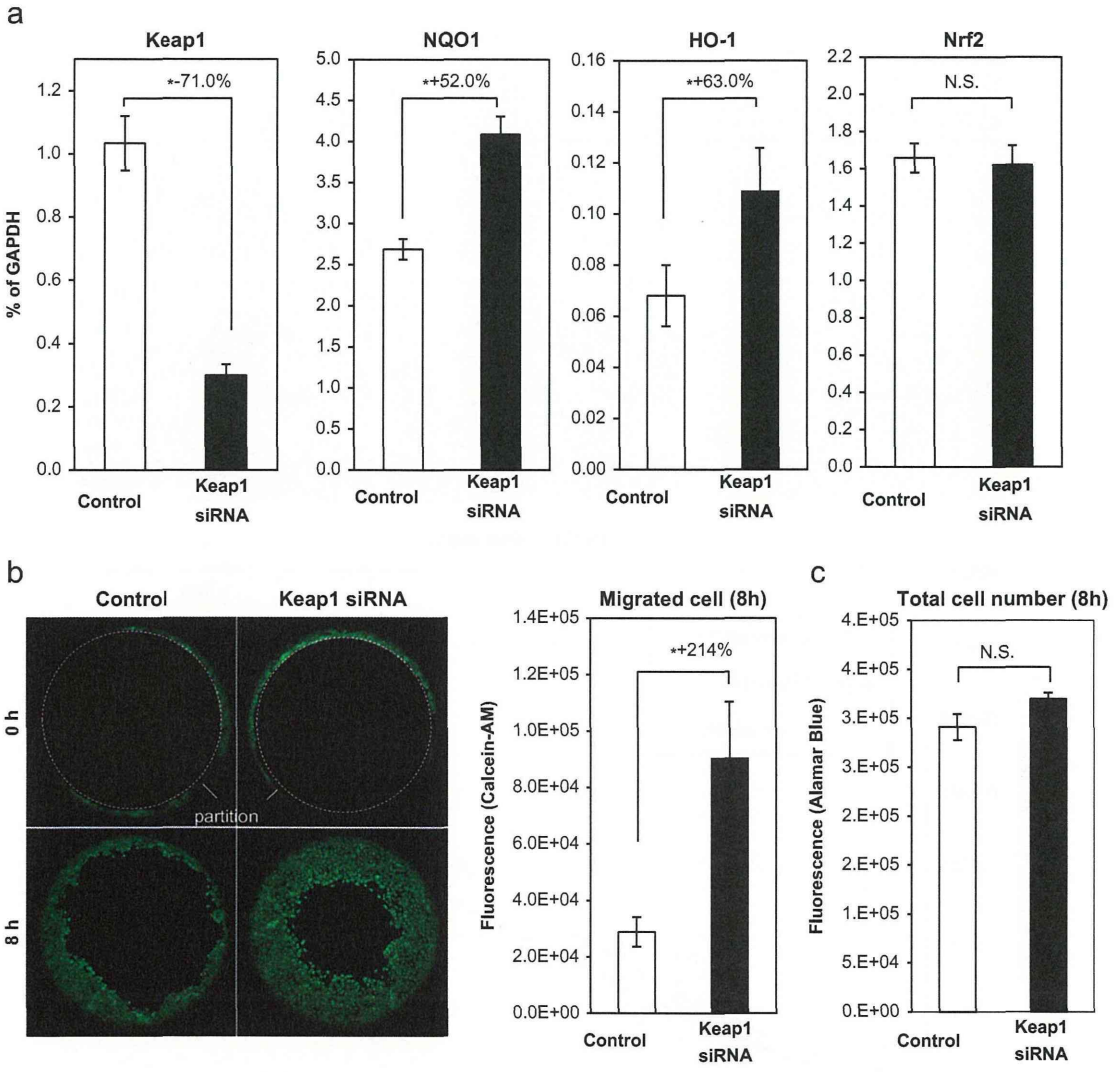

Fig. 6. The effect of Keap1 knockdown on the migration capability of corneal epithelial cells in vitro. (a) The effects of Keap1-specific knockdown on the migration capability of C/TERT cells were examined; 71.0% of Keap1 mRNA expression in C/TERT cells was suppressed by Keap1-specific siRNA. Keap1 knockdown significantly upregulated the expression of NQO1 (52.0%) and HO-1 (60.3%) but not Nrf2. (b) Keap1- or control siRNA-introduced cells were allowed to migrate for 8 h and then stained with calcein-AM. Migration assay indicated that the cell-migration capability was significantly promoted by Keap1 knockdown. (c) The Alamar blue assay revealed no significant effect of Keap1 knockdown on cell numbers. The graphs represent the means ± SE of four independent samples. $*p < 0.05$ (t test).

Effect of Nrf2 suppression or activation by siRNA on proliferative capability of corneal epithelial cells

To evaluate whether the Nrf2/Keap1 system was involved in corneal epithelial proliferation, we investigated the proliferation profiles of Nrf2 and Keap1 knockdown C/TERT cells. Nrf2 suppression by siRNA had no significant effect on the proliferative capability of C/TERT (Fig. 7). The proliferation of C/TERT cells seemed to be slightly decreased by Nrf2 activation caused by Keap1 knockdown, but the decrease was not significant throughout the cell culture periods up to 72 h.

Discussion

The aim of this study was to clarify the role of the Nrf2-mediated defense system in corneal epithelial wound healing by using Nrf2 KO mice.

To first assess the involvement of Nrf2 in corneal epithelial wound healing in WT and Nrf2 KO mice, the corneal epithelia of mice from each group were injured by *n*-heptanol treatment. The HE and fluorescein staining showed that the *n*-heptanol treatment completely removed the corneal epithelial cell layer and that no inflammatory cells invaded the corneal tissue during wound healing. This finding suggests that the wound-healing process in this model is relatively simple, occurring without the involvement of inflammatory cells.

The results of the experiment using this model demonstrated that wound healing in the KO mice was significantly delayed for 24–48 h after injury. The results of HE staining during the process of corneal wound healing revealed that during the first 12–24 h after the injury, epithelial migration in Nrf2 KO mice was apparently delayed compared to that in the WT mice. Interestingly, 24–36 h after injury, the total number of Ki-67-positive corneal epithelial cells in the KO mice decreased significantly compared to that in the WT mice. These data suggest that the delay in wound healing in the KO mice resulted from decreased cell proliferation. However, the number of Ki-67-positive cells in the KO mice recovered to the same levels as in the WT mice by 48 h after injury. The process of corneal epithelial wound healing generally